Core dynamo simulations of A-type stars

Master's thesis project

Juan Pablo Hidalgo

Supervisor : Dr. Dominik Schleicher

Universidad de Concepción.

September 20, 2023

Stellar structure

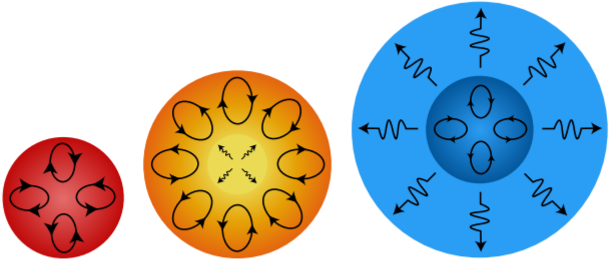

Figure: Diagram of convective and radiative zones for different ranges of stellar masses. Stars with $M \lesssim 0.3 M_\odot$ are fully convective, intermediate mass stars have a radiative core and a convective core. Finally, stars with $M \gtrsim 1.5 M_\odot$ have convective cores and radiative envelopes.

Stellar structure

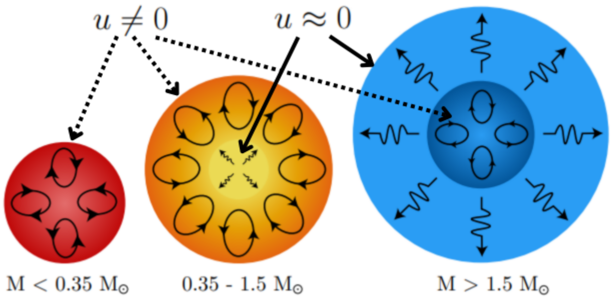

Figure: Diagram of convective and radiative zones for different ranges of stellar masses. Stars with $M \lesssim 0.3 M_\odot$ are fully convective, intermediate mass stars have a radiative core and a convective core. Finally, stars with $M \gtrsim 1.5 M_\odot$ have convective cores and radiative envelopes.

Astrophysical Dynamos

We refer to a *dynamo* as any process of amplification and maintenance of magnetic fields inside a plasma.

$$\frac{\partial \vec{B}}{\partial t} = \vec{\nabla} \times (\vec{u} \times \vec{B}) + \eta \nabla^2 \vec{B}$$

These processes are most likely to occur inside the convection zones (see Brandenburg & Subramanian 2004), where $u \neq 0$.

Radiative zone?

Ap/Bp stars (1.5 $M_\odot$ to $6M_\odot$) host magnetic fields with mean strengths ranging from 200 G to 30 kG (Aurière et al., 2007).

Possible explanations

The dynamo is driven by the convective core of the star (Krause & Oetken, 1976).

Possible explanations

The dynamo is driven by the convective core of the star (Krause & Oetken, 1976).

Previous work

Brun et al. (2005) performed simulations of the inner 30% by radius (where 15% is the core) of a $2\ M_{\odot}$ A-type star, obtaining magnetic fields with typical strengths around the equipartition values with the kinetic energy.

Possible explanations (2)

Surface magnetic field?

In principle, magnetic structures created by the core dynamo could reach the surface under the action of buoyancy, however, this process has a timescale longer than the main-sequence life of the star (Parker, 1979; Moss, 1989), unless we consider very small structures (MacGregor & Cassinelli, 2003).

Possible explanations (3)

Fossil field surviving from the early stages (Cowling, 1945).

Possible explanations (3)

Fossil field surviving from the early stages (Cowling, 1945).

Previous work

Braithwaite & Nordlund (2005) performed 3D simulations of a $2M_\odot$, $R = 1.8R_\odot$ A-type star, inside a box of side $l = 4.5R$ using a grid of 96^3. They found stable axisymmetric magnetic field configurations in a radiative interior starting with random field initial conditions. Recently, similar results were found by Becerra et al. (2022).

Possible explanations (4)

Survival of fossil fields during the pre-main sequence evolution of intermediate-mass stars

Dominik R.G. Schleicher[1], Juan Pablo Hidalgo[1], and Daniele Galli[2]

[1] Departamento de Astronomía, Facultad Ciencias Físicas y Matemáticas, Universidad de Concepción, Av. Esteban Iturra s/n,Barrio Universitario, Concepción, Chile. e-mail: dschleicher@astro-udec.cl
[2] INAF - Osservatorio Astrofisico di Arcetri, Largo E. Fermi 5, 50125 Firenze, Italy

June 30, 2023

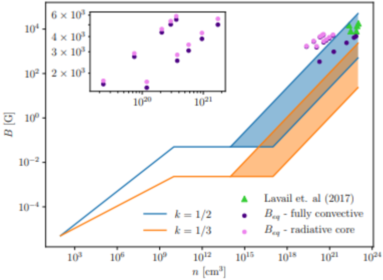

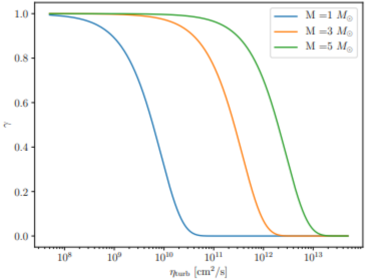

Main-sequence model

In this project, we performed 3D MHD simulations of an A-type star with a radiative envelope and a convective core assumed to encompass 20% of the stellar radius (similar to Brun et al. 2005 and Featherstone et al. 2009)

Objectives:

- Analyze the dynamo solutions given by the core, and possible surface magnetic fields.

Main-sequence model

In this project, we performed 3D MHD simulations of an A-type star with a radiative envelope and a convective core assumed to encompass 20% of the stellar radius (similar to Brun et al. 2005 and Featherstone et al. 2009)

Objectives:

- Analyze the dynamo solutions given by the core, and possible surface magnetic fields.
- Study the large scale flows in the core of the star.

Main-sequence model

In this project, we performed 3D MHD simulations of an A-type star with a radiative envelope and a convective core assumed to encompass 20% of the stellar radius (similar to Brun et al. 2005 and Featherstone et al. 2009)

Objectives:

- Analyze the dynamo solutions given by the core, and possible surface magnetic fields.
- Study the large scale flows in the core of the star.
- Compare these results with previous work showed before.

The setup

Using The PENCIL CODE (Pencil Code Collaboration et al., 2021), we model a massive early-type star of radius R, inside a box of side $l = 2.2R$.

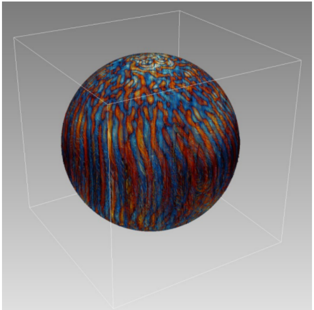

Figure: Star-in-a-box model, from Käpylä (2021).

Stellar parameters:

$$R_* = 2R_\odot$$
$$L_* = 23L_\odot$$
$$\rho_* = 5.6 \cdot 10^4 \text{ g/m}^3$$
$$g_* = 150 \text{ m/s}^2$$

The model

Solving the fully-compressible non-ideal MHD equations:

$$\frac{\partial \vec{A}}{\partial t} = \vec{u} \times \vec{B} - \eta\mu_0 \vec{J} \tag{1}$$

$$\frac{D \ln \rho}{Dt} = -\vec{\nabla} \cdot \vec{u} \tag{2}$$

$$\frac{D\vec{u}}{Dt} = -\vec{\nabla}\Phi - \frac{1}{\rho}\left(\vec{\nabla}p - \vec{\nabla} \cdot 2\nu\rho\boldsymbol{S} + \vec{J} \times \vec{B}\right) - 2\vec{\Omega} \times \vec{u} + \vec{f}_d \tag{3}$$

$$T\frac{Ds}{Dt} = -\frac{1}{\rho}\left[\vec{\nabla} \cdot (\vec{F}_{\mathrm{rad}} + \vec{F}_{\mathrm{SGS}}) + \mathcal{H} - \mathcal{C}\right] + 2\nu\boldsymbol{S}^2 + \mu_0\eta J^2 \tag{4}$$

where $D/Dt = \partial/\partial t + \vec{u} \cdot \vec{\nabla}$ is the advective derivative, also $\vec{B} = \vec{\nabla} \times \vec{A}$, the relation between $\vec{J}$ and $\vec{B}$ is given by the Ohm's law $\vec{J} = \vec{\nabla} \times \vec{B}/\mu_0$ and the explicit heating and cooling terms, are extracted from Käpylä (2021).

Simulations

MHD simulations have a radial profile in the diffusivities, with $r_{\text{start}} = 0.35R$ and $w = 0.06R$.
* indicates $r_{\text{start}} = 0.30R$ and $w = 0.03R$.

Run	P_{rot} [days]	$\langle u_{\text{rms}} \rangle$ [m/s]	$\langle B_{\text{rms}} \rangle$ [kG]	Co	Re	Re_{M}
MHDr1	20	179	no dynamo	1.8	146	102
MHDr2	15	82	113	5.3	67	47
MHDr2*	15	80	114	5.4	65	46
MHDr3	10	62	111	10.4	51	36
MHDr3*	10	61	122	10.7	50	35
MHDr4	8	56	110	14.4	46	32
MHDr4*	8	56	103	14.5	46	32

$$\text{Re} = \frac{u_{\text{rms}}}{\nu k_R} \qquad \text{Re}_{\text{M}} = \frac{u_{\text{rms}}}{\eta k_R} \qquad \text{Co} = \frac{2\Omega_0}{u_{\text{rms}} k_R}$$

Analysis

All the analysis in this work, was made during the thermally and magneticaly relaxation of the runs.

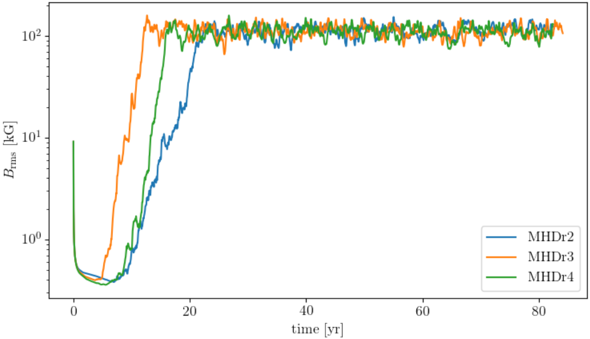

Figure: Time evolution of the volume-averaged root-mean-square magnetic field, from the runs in MHD group that generate core dynamos.

Dynamo solutions

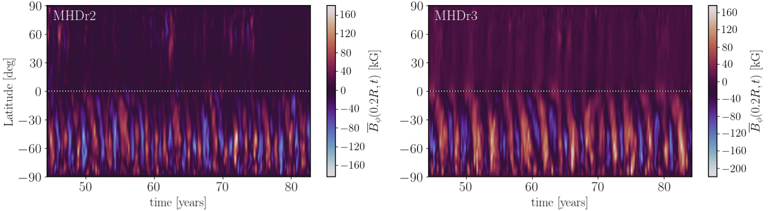

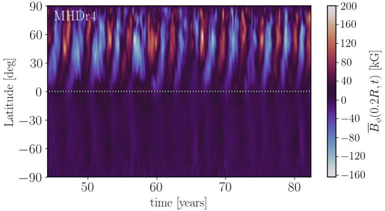

Run	$\overline{B}_\phi^{\rm min}$	$\overline{B}_\phi^{\rm rms}$	$\overline{B}_\phi^{\rm max}$
MHDr2	-182.1	31.6	178.0
MHDr3	-216.9	35.2	175.7
MHDr4	-162.0	35.8	197.9

Figure: Time-latitude diagrams of the azimuthally averaged toroidal magnetic field $\overline{B}_\phi(r = 0.2R, \theta, t)$ of the MHD group.

Dynamo solutions (2)

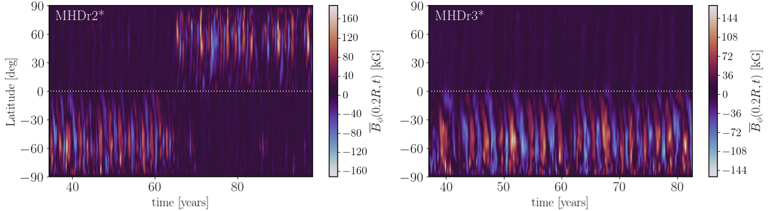

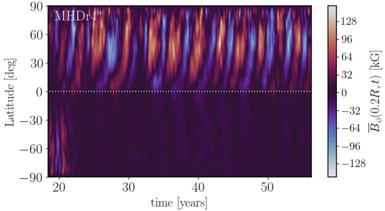

Run	$\overline{B}_\phi^{\min}$	$\overline{B}_\phi^{\mathrm{rms}}$	$\overline{B}_\phi^{\max}$
MHDr2*	-171.7	30.0	185.0
MHDr3*	-152.5	29.2	164.7
MHDr4*	-150.7	31.8	152.4

Figure: Time-latitude diagrams of the azimuthally averaged toroidal magnetic field $\overline{B}_\phi(r = 0.2R, \theta, t)$ of the MHD* group.

Comparison with other simulations

The Astrophysical Journal Letters, 902:L3 (6pp), 2020 October 10 https://doi.org/10.3847/2041-8213/abb9a4

CrossMark

Single-hemisphere Dynamos in M-dwarf Stars

Benjamin P. Brown[1], Jeffrey S. Oishi[2], Geoffrey M. Vasil[3], Daniel Lecoanet[4], and Keaton J. Burns[5,6]
[1] Department Astrophysical and Planetary Sciences & LASP, University of Colorado, Boulder, CO 80309, USA; bpbrown@colorado.edu
[2] Department of Physics and Astronomy, Bates College, Lewiston, ME 04240, USA
[3] School of Mathematics and Statistics, University of Sydney, Sydney, NSW 2006, Australia
[4] Department of Engineering Science and Applied Mathematics, Northwestern University, 2145 Sheridan Road, Evanston, IL 60208, USA
[5] Department of Mathematics, Massachusetts Institute of Technology, Cambridge, MA 02139, USA
[6] Center for Computational Astrophysics, Flatiron Institute, New York, NY 10010, USA
Received 2020 August 4; revised 2020 September 11; accepted 2020 September 17; published 2020 October 7

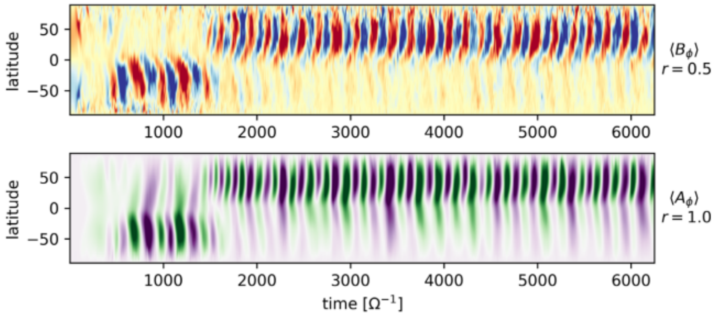

Comparison with other simulations (2)

Simulations of dynamo action in slowly rotating M dwarfs: Dependence on dimensionless parameters

C. A. Ortiz-Rodríguez[1], P. J. Käpylä[2,3,4], F. H. Navarrete[5,4], D. R. G Schleicher[1], R. E. Mennickent[1], J.P. Hidalgo[1], and B. Toro[1]

[1] Departamento de Astronomía, Facultad de Ciencias Físicas y Matemáticas, Universidad de Concepción, Av. Esteban Iturra s/n Barrio Universitario, Casilla 160-C, Chile
[2] Leibniz-Institut für Sonnenphysik (KIS), Schöneckstr. 6, 79104 Freiburg, Germany
[3] Institut für Astrophysik und Geophysik, Georg-August-Universität Göttingen, Friedrich-Hund-Platz 1, 37077 Göttingen, Germany
[4] Nordita, KTH Royal Institute of Technology and Stockholm University, 10691 Stockholm, Sweden
[5] Hamburger Sternwarte, Universität Hamburg, Gojenbergsweg 112, 21029 Hamburg, Germany

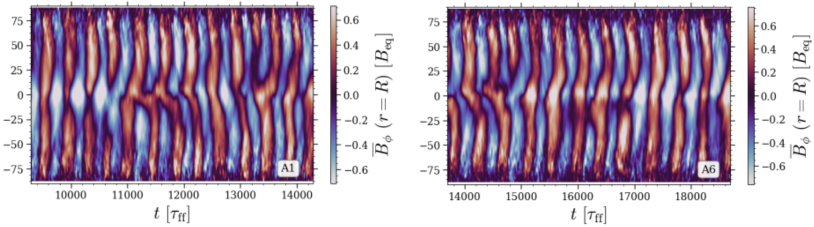

Surface magnetic fields

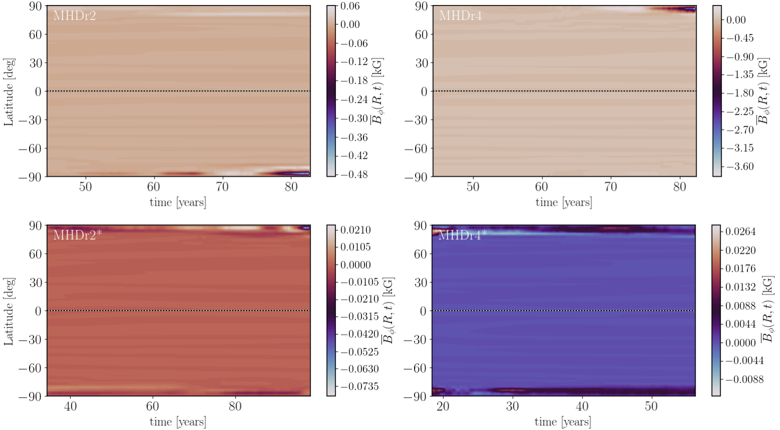

Figure: Time-latitude diagrams of the azimuthally averaged toroidal magnetic field $\overline{B}_\phi(r = R, \theta, t)$ of both groups.

Large-scale flows

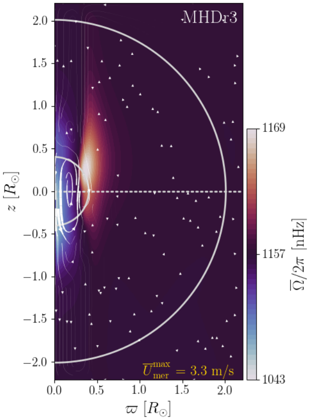

Figure: Profile of the temporally and azimuthally averaged rotation rate $\overline{\Omega}(\varpi, z)$ for MHDr3. The streamlines indicate the mass flux due to meridional circulation and the maximum averaged meridional flow is indicated in the lower left side of each plot.

Large-scale flows (2)

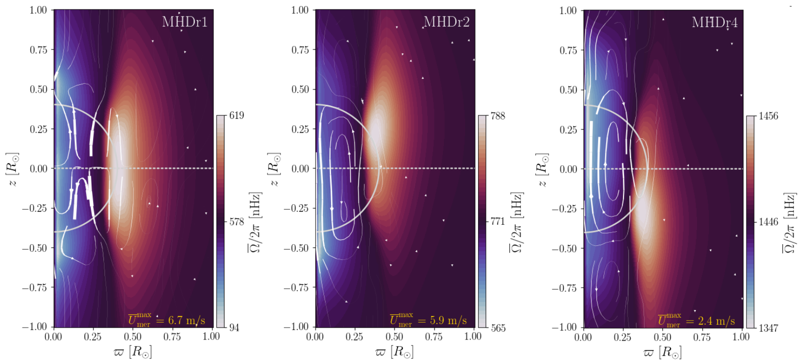

Figure: Profiles of the temporally and azimuthally averaged rotation rate $\overline{\Omega}(\varpi, z)$ for runs from the MHD group. The streamlines indicate the mass flux due to meridional circulation and the maximum averaged meridional flow is indicated in the lower left side of each plot.

Large-scale flows (3)

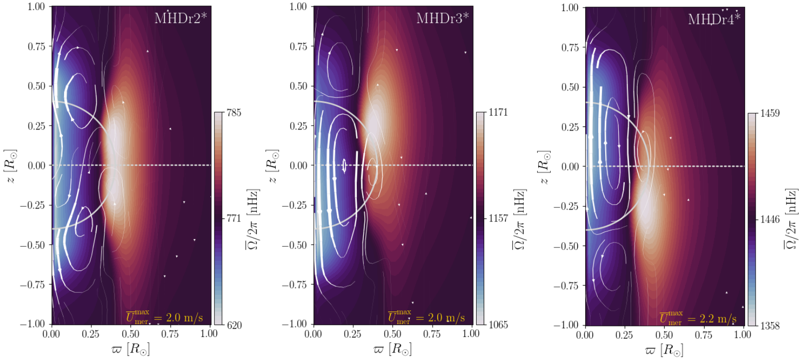

Figure: Profiles of the temporally and azimuthally averaged rotation rate $\overline{\Omega}(\varpi, z)$ for runs from the MHD* group. The streamlines indicate the mass flux due to meridional circulation and the maximum averaged meridional flow is indicated in the lower left side of each plot.

Energy analysis

From the time series, we have $E_{\text{mag}} = \int_V \frac{1}{2\mu_0}\mathbf{B}^2 dV$ and $E_{\text{kin}} = \int_V \frac{1}{2}\rho\mathbf{u}^2 dV$. Plotting these quantities:

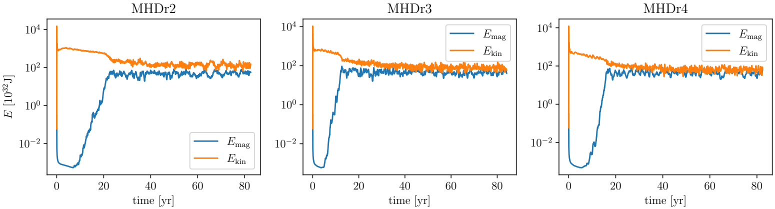

Figure: Temporal evolution of magnetic and kinetic energy from group MHD.

To conclude

Conclusions

- The core of the star is able to produce very strong magnetic fields ($\overline{B}_\phi \sim 200$ kG).

To conclude

Conclusions

- The core of the star is able to produce very strong magnetic fields ($\overline{B}_\phi \sim 200$ kG).
- A core dynamo does not seem to be sufficient to explain the large-scale magnetic fields of Ap stars.

To conclude

Conclusions

- The core of the star is able to produce very strong magnetic fields ($\overline{B}_\phi \sim 200$ kG).
- A core dynamo does not seem to be sufficient to explain the large-scale magnetic fields of Ap stars.
- These fields have roughly equipartition values in fast rotators, similar to Brun et al. (2005) and Featherstone et al. (2009).

To conclude

Conclusions

- The core of the star is able to produce very strong magnetic fields ($\overline{B}_\phi \sim 200$ kG).
- A core dynamo does not seem to be sufficient to explain the large-scale magnetic fields of Ap stars.
- These fields have roughly equipartition values in fast rotators, similar to Brun et al. (2005) and Featherstone et al. (2009).
- Vertical flows might be transporting the magnetic field to the surface, due to the high Coriolis number.

To conclude

Conclusions

- The core of the star is able to produce very strong magnetic fields ($\overline{B}_\phi \sim 200$ kG).
- A core dynamo does not seem to be sufficient to explain the large-scale magnetic fields of Ap stars.
- These fields have roughly equipartition values in fast rotators, similar to Brun et al. (2005) and Featherstone et al. (2009).
- Vertical flows might be transporting the magnetic field to the surface, due to the high Coriolis number.
- The envelope has approximately-rigid rotation like the radiative interior of the Sun (see Howe 2009). And the core has solar-like differential rotation in all runs.

Future work

Next steps

- Explore more rotation rates.

Future work

Next steps

- Explore more rotation rates.
- Study how a fossil field would affect the nature of the core dynamo.

Future work

Next steps

- Explore more rotation rates.
- Study how a fossil field would affect the nature of the core dynamo.
- Are these two elements enough to explain the large-scale magnetic fields of Ap/Bp stars?

References I

Aurière M., et al., 2007, A&A, 475, 1053

Becerra L., Reisenegger A., Valdivia J. A., Gusakov M. E., 2022, MNRAS, 511, 732

Braithwaite J., Nordlund A., 2005, Astronomy and Astrophysics, 450

Brandenburg A., Subramanian K., 2004, Phys. Rep., 417

Brun A. S., Browning M. K., Toomre J., 2005, ApJ, 629, 461

Cowling T. G., 1945, MNRAS, 105, 166

Featherstone N. A., Browning M. K., Brun A. S., Toomre J., 2009, ApJ, 705, 1000

Howe R., 2009, Living Reviews in Solar Physics, 6, 1

Käpylä P. J., 2021, A&A, 651, A66

Krause F., Oetken L., 1976, in Weiss W. W., Jenkner H., Wood H. J., eds, IAU Colloq. 32: Physics of Ap Stars. p. 29

Käpylä P. J., Gent F. A., Olspert N., Käpylä M. J., Brandenburg A., 2020, Geophysical & Astrophysical Fluid Dynamics, 114, 8

Lyra W., McNally C. P., Heinemann T., Masset F., 2017, AJ, 154, 146

MacGregor K. B., Cassinelli J. P., 2003, ApJ, 586, 480

Moss D., 1989, MNRAS, 236, 629

Parker E. N., 1979, Ap&SS, 62, 135

Pencil Code Collaboration et al., 2021, The Journal of Open Source Software, 6, 2807

Physical Units

The Pencil Code expresses all the relevant quantities in code units, so to give them physical meaning it is required to do some conversions:

$$[x] = \left(\frac{R_*}{R_{\rm sim}}\right) \qquad [t] = \left(\frac{\Omega_{\rm sim}}{\Omega_*}\right)$$

$$[u] = \left(\frac{\Omega_* R_*}{\Omega_{\rm sim} R_{\rm sim}}\right) \qquad [B] = \left[\frac{\mu_0 \rho_* (\Omega_* R_*)^2}{\mu_{\rm sim} \rho_{\rm sim} (\Omega_{\rm sim} R_{\rm sim})^2}\right]^{1/2}$$

where (see Appendix A of Käpylä et al. 2020):

$$\frac{\Omega_{\rm sim}}{\Omega_*} = L_{\rm ratio}^{1/3} \left(\frac{g_{\rm sim}}{g_*}\frac{R_*}{R_{\rm sim}}\right)^{1/2}$$

Schwarzschild criterion

According to the Schwarzschild criterion, we can expect convection to occur if:

$$\vec{\nabla}_{\rm rad} = \frac{3}{16\pi acG}\frac{P}{T^4}\frac{\kappa l}{m} > \vec{\nabla}_{\rm ad}$$

This is:

- A large value of the opacity κ. Since low-mass stars are cooler than high-mass stars, we may expect low-mass stars to have convective envelopes.
- Regions with a large energy flux (i.e. large l/m), stars which nuclear energy production is strongly peaked towards the centre can be expected to have convective cores.

Hyper-diffusivities

The code offers numerical sixth-order tools which smooths out the smallest scales, dissipating the energy and preventing instabilities. Here, we used the mesh method implemented by Alex Brandenburg described in Lyra et al. (2017):

$$f_{\rm visc}^{\rm (hyper)} = \nu_3^{\rm mesh} \frac{\Delta^6 \nu}{\Delta q^6}, \qquad f_{\rm diff}^{\rm (hyper)} = \eta_3^{\rm mesh} \frac{\Delta^6 \eta}{\Delta q^6}$$

Differential rotation (2)

The differential rotation is studied using the following parameters:

$$\Delta_\Omega^{(r)} = \frac{\overline{\Omega}(r_{\rm top}, \theta_{\rm eq}) - \overline{\Omega}(r_{\rm bot}, \theta_{\rm eq})}{\overline{\Omega}(r_{\rm top}, \theta_{\rm eq})},$$

$$\Delta_\Omega^{(\overline{\theta})} = \frac{\overline{\Omega}(r_{\rm top}, \theta_{\rm eq}) - \overline{\Omega}(r_{\rm top}, \overline{\theta})}{\overline{\Omega}(r_{\rm top}, \theta_{\rm eq})},$$

where $r_{\rm top} = 0.9R$ and $r_{\rm bot} = 0.1R$ are the radius at the top and bottom of the star, respectively. $\overline{\theta}$ is an average of $\overline{\Omega}$ between latitudes $-\theta$ and θ.

Differential rotation (3)

Run	$\Delta_\Omega^{\mathrm{CZ}(r)}$	$\Delta_\Omega^{\mathrm{CZ}\bar{\theta}}(60°)$	$\Delta_\Omega^{\mathrm{CZ}\bar{\theta}}(75°)$	$\Delta_\Omega^{(r)}$	$\Delta_\Omega^{\bar{\theta}}(60°)$	$\Delta_\Omega^{\bar{\theta}}(75°)$
MHDr2	0.1131	0.0699	0.1142	0.0505	-0.0001	-0.0006
MHDr2*	0.1101	0.0683	0.1133	0.0485	-0.0001	-0.0006
MHDr3	0.0538	0.0295	0.0484	0.0251	-0.0000	-0.0004
MHDr3*	0.0489	0.0283	0.0438	0.0224	-0.0001	-0.0006
MHDr4	0.0405	0.0213	0.0350	0.0197	-0.0000	-0.0003
MHDr4*	0.0387	0.0208	0.0333	0.0169	-0.0001	-0.0006

Figure: Differential rotation parameters for all simulations, obtained from the averaged (azimuthally and temporally) angular velocity $\overline{\Omega}$.

The radiative envelope has almost rigid rotation, and the core has solar-like rotation in all runs.

Initial conditions

The convective core is assumed to encompass 20% of the stellar radius (similar to Brun et al. 2005 and Featherstone et al. 2009).

We assumed a piecewise polytropic initial state: $p(\rho) = K_0 \rho^{\gamma}$, where $\gamma = 1 + \frac{1}{n}$, and:

$$n = \begin{cases} 1.5 & \text{if} \quad r < 0.2R \\ 3.25 & \text{if} \quad r > 0.2R \end{cases},$$

is the polytropic index.

Possible explanations (4)

Interaction between a core dynamo and a fossil field.

Previous work

Featherstone et al. (2009) performed 3D simulations of the inner 30% by radius of a $2M_\odot$ A-type star (excluding the innermost values), modeling a core dynamo surrounded by a radiative envelope. The inclusion of a fossil field in this envelope can lead to a very strong super-equipartition field.

Possible explanations (6)

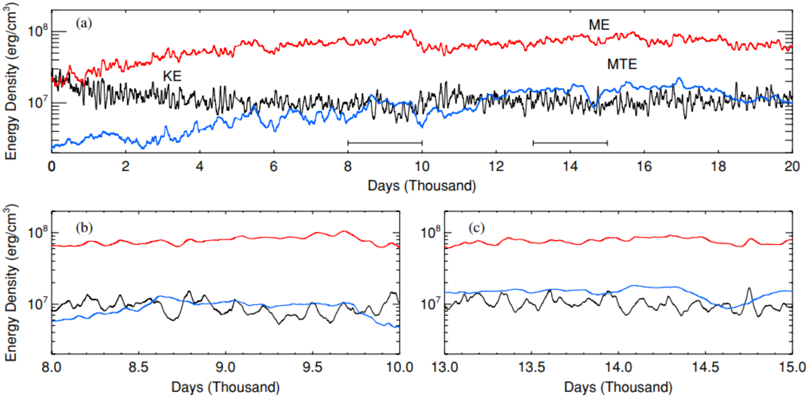

Figure: Temporal evolution of overall energy densities after imposing a mixed poloidal–toroidal magnetic (fossil) field configuration. The magnetic energy (ME) grows until it reaches 10 times the value of the kinetic energy (KE). Extracted from Featherstone et al. (2009).